Unified Optical-Thermal Four-Stream Radiative Transfer Theory for Homogeneous Vegetation Canopies

Wout Verhoef, Li Jia, Qing Xiao, and Z. Su

***Abstract*—Foliage and soil temperatures are key variables for assessing the exchanges of turbulent heat fluxes between vegetated land and the atmosphere. Using multiple-view-angle thermal-infrared (TIR) observations, the temperatures of soil and vegetation may be retrieved. However, particularly for sparsely vegetated areas, the soil and vegetation component temperatures in the sun and in the shade may be very different depending on the solar radiation, the physical properties of the surface, and the meteorological conditions. This may interfere with a correct retrieval of component temperatures, but it might also yield extra information related to canopy structure. Both are strong reasons to investigate this phenomenon in some more detail. To this end, the relationship between the TIR radiance directionality and the component temperatures has been analyzed. In this paper, we extend the four-stream radiative transfer (RT) formalism of the Scattering by Arbitrarily Inclined Leaves model family to the TIR domain. This new approach enables us to simulate the multiple scattering and emission inside a geometrically homogenous but thermodynamically heterogeneous canopy for optical as well as thermal radiation using the same modeling framework. In this way top-of-canopy thermal radiances observed under multiple viewing angles can be related to the temperatures of sunlit and shaded soil and sunlit and shaded leaves. In this paper, we describe the development of this unified optical-thermal RT theory and demonstrate its capabilities. A preliminary validation using an experimental data set collected in the Shunyi remote sensing field campaign in China is briefly addressed.**

***Index Terms*—Component temperature, directional emissivity, radiative transfer (RT) model, scattering by arbitrarily inclined leaves (SAIL), surface temperature, thermal-infrared (TIR) radiation.**

Manuscript received March 29, 2006; revised August 14, 2006. This work was supported in part by the National Aerospace Laboratory's own Research Program; by the European Space Agency (ESA), ESTEC Contract 17179/03/NL/GS, Validation of the Surface Processes and Ecosystem Changes Through Response Analysis (SPECTRA) Mission Concept using Earth System Models and Land Surface Experiments, led by Dr. M. Menenti, with Dr. M. Rast as the ESA Study Manager; by an Instituto de Astrofisica de Canarias (IAC) fellowship from the Netherlands Ministry of Agriculture, Nature Management, and Fisheries; by the Netherlands Users' Support Program (SRON GO) under Grant EO-049, with Dr. R. de Groot as the SRON GO Program Manager; by the EC FP6 GMES EAGLE Project, Contract 502057, led by Prof. J. A. Sobrino, with Dr. P. Breger as the EC Project Officer; and by China's Special Funds for Major State Basic Research, Project G2000077900, led by Prof. X. Li, for the Shunyi field campaign, part of the "Quantitative of Remote Sensing theory and application for Land Surface Parameters (QRSLSP)" Project.

W. Verhoef is with the National Aerospace Laboratory, Emmeloord, The Netherlands (e-mail: verhoef@nlr.nl).

L. Jia is with Alterra Green World Research, Wageningen University and Research Center, Wageningen, The Netherlands.

Q. Xiao is with Beijing Research Institute of Uranium Geology, China National Nuclear Corporation, Beijing, China.

Z. Su is with the International Institute for Geo-Information Science and Earth Observation ITC, Enschede, The Netherlands.

Digital Object Identifier 10.1109/TGRS.2007.895844

I. Introduction

OPTICAL radiative transfer (RT) models of various types have been developed in the past [1], [2] to describe the scattering and absorption of radiation inside agricultural leaf canopies and forests. These models can be applied in order to enhance the understanding of remotely sensed images of the vegetation on Earth and to support the quantitative use of remote sensing data by the design of algorithms for the retrieval of biophysical parameters. Although there are various degrees of overlap among existing models, they can roughly be grouped in geometric optics (GO), RT, and hybrid (GORT) models, in which both approaches are combined. GO models describe vegetation canopy RT by means of simplified opaque subcanopies of various geometric shapes, i.e., cubic, cylindrical, conical, and ellipsoidal. RT models put more emphasis on the directional scattering and absorption of radiation by canopy elements like leaves or needles, which can be accomplished by means of various analytical and numerical approaches, such as four stream [3], [4], discrete ordinates [5], [6], radiosity [7], ray tracing [8], Monte Carlo [9], and successive orders of scattering [10]. In particular, 3-D modeling approaches rely on numerical techniques and are also more suitable to be combined with GO modeling [11], [12], thus leading to the GORT category of models [13]–[15]. Parallel to these physically based models, there are also models which only describe the angular signature of the bidirectional properties by mathematical kernels. These models are called parametric models [16]–[18].

More or less independent of these optical models, other models have been developed for application to thermal infrared (TIR) imagery to simulate the radiometric temperature of canopy–soil combinations. These modeling studies on the directionality properties of TIR radiance of vegetation canopies can be grouped into the same prevailing categories as the optical models according to model development principles, i.e., simple GO and RT models. While GO models [19]–[23] are suitable to model clumped (forestry) or row-structured canopies, the physical processes included in these models are mostly limited. RT models involve various degrees of detail in physical processes, characterizing the vegetation canopy by a leaf density distribution [or only total leaf area index (LAI)], a leaf inclination distribution function (LIDF), etc., and often assuming canopies as homogeneous turbid media composed of layers with different temperatures, which are either given as input or solved simultaneously [24]–[30]. Many TIR RT models are indeed hybrid GO and RT (GORT) models, which

combine RT theories (as in RT models) and canopy geometric constructions (as in pure GO models) with various emphases on either aspects. In [31]–[33], gap probabilities and RT are considered for homogeneous and row-structured crops. Among the published TIR RT or GORT models, few studies (e.g., [34]) have taken account of temperature differences between sunlit and shaded soil and sunlit and shaded leaves, which, however, may be significant for an incomplete canopy, depending on the solar radiation, the physical state of the surface, and the meteorological conditions.

With computer technology developing rapidly, some numerically based models have been proposed to simulate TIR scenes of 3-D canopies (e.g., [35]). This type of model is usually capable of representing the 3-D nature of a canopy in a relatively precise manner, providing that canopy structure is known beforehand. For instance, thermal heterogeneity of a canopy resulting from the contrast of sunlit/shaded leaves and soil may be better described by a 3-D model than by any complicated 1-D RT model. It requires, however, many parameters to define the 3-D geometric structure of a canopy, which makes it difficult to deal with the inversion problem.

As yet, very few studies have been reported on concurrently dealing with RT within vegetation canopies in the optical domain and in the TIR domain in one canopy model, although there are obvious benefits, since they can share a common architectural description. In [36], an optical parametric bidirectional reflectance distribution function (BRDF) model is applied to the TIR in order to compute directional emissivities using Kirchhoff's Law. A similar approach is followed in [37] for nonisothermal surfaces. The 3-D discrete anisotropic radiative transfer (DART) model [15] has been applied to the thermal domain [35] as well, and some of their results are discussed in Section III of this paper.

In this paper, we explore the possibility of applying the Scattering by Arbitrarily Inclined Leaves (SAIL) family [4], [38] of canopy RT models to the TIR domain. This enables us to partly bridge the current gap between the analytical canopy–soil models operating separately in the optical and the TIR spectral domains, and it might lead to better exploitation of the possible synergies offered by simultaneous coregistered optical and TIR remote sensing observations, such as would have been provided by the former candidate European Space Agency (ESA) mission Surface Processes and Ecosystem Changes Through Response Analysis (SPECTRA). An additional advantage is that, in such a unified model, a common description of canopy architecture is applied for both spectral domains, so that one might be able to devise advanced methods to retrieve canopy structure along with accurate component temperatures. In this paper, we will focus on the applicability of the four-stream RT theory to homogeneous vegetation canopies when thermal emission of radiation by leaves and the soil is incorporated. Section II gives some insight in the theoretical developments. We demonstrate the capabilities of the new approach for thermal simulations in Section III, including comparisons with several other models and discussions. A preliminary validation of the four-stream unified model is performed using an experimental directional TIR data set collected in the Shunyi field campaign in China in 2001 [39], [40]. We include a discussion of the results in Section IV. The conclusions are drawn in the last section.

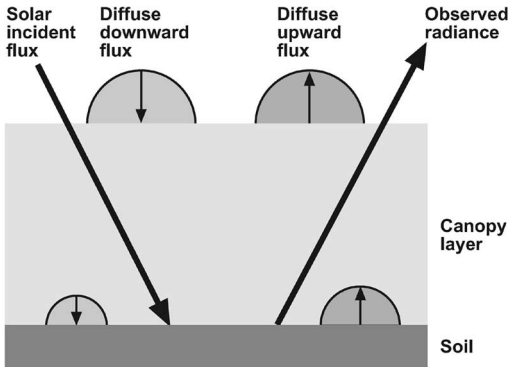

Fig. 1. Four-stream RT modeling concept as applied in Suits and SAIL models.

II. Theory

The SAIL canopy reflectance model was developed in the early 1980s [41] as a refinement of the model of Suits [3]. To relieve the restriction of the Suits model to exclusively horizontal and vertical leaf facets, a leaf inclination distribution function was introduced in SAIL in order to express the scattering and extinction coefficients of the canopy as a function of this LIDF, angular geometry, and leaf optical properties. In [4], the derivation of these coefficients is described in detail, and some examples of simulated directional reflectance profiles are shown. Both the Suits and the SAIL model are examples of four-stream representations (Fig. 1) of the RT equation, in which case one distinguishes two direct fluxes (incident solar flux and radiance in the viewing direction) and two diffuse fluxes (upward and downward hemispherical flux). The interactions of these fluxes with the canopy are described by a system of four linear differential equations, which can be analytically solved. Initially, this was accomplished by formulating a general solution and then solving the boundary equations resulting from the incident fluxes at the top and the bottom of the canopy layer, via the soil's reflectance. This boundary equation method requires explicit knowledge of the fraction of diffuse incident flux (skylight) and of the soil's reflectance in order to be able to solve the linear system of equations. In [42], a more flexible method was introduced by application of the adding method [43]. In the adding method, all reflected and transmitted fluxes of a canopy layer are expressed in all possible fluxes incident to that layer. The interaction of the canopy layer with the incident radiation from the sun and the sky, and with the soil background, is described by means of a series of fundamental reflectance and transmittance quantities (bihemispherical, hemispherical-directional, directional-hemispherical, and bidirectional), which were all referring to the isolated canopy layer. By means of this versatile method, one can build up arbitrarily complex ensembles of different canopy layers on a soil background, which is not necessarily Lambertian, and then compute the bidirectional reflectance at the top-of-canopy (TOC) level. In addition, the interaction of the atmosphere with the Earth's surface can be conveniently described using the

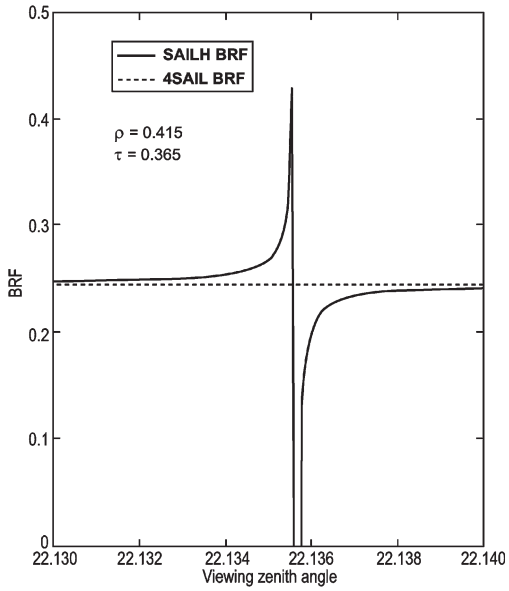

Fig. 2. Numerical instability in SAILH model and corresponding smooth output of model 4SAIL, in which this singularity is properly intercepted.

same terminology. Incorporation of the foliage hotspot effect in SAIL was accomplished in 1989 and resulted in the model called SAILH [38]. In SAILH, the single scattering contribution to the bidirectional reflectance was modified according to the theory of Kuusk [44], while all other terms remained the same. A detailed description of this modification is given in [38].

The analytical solution method applied in the earlier SAIL models can lead to numerical problems if certain mathematical singularities that might occur under particular conditions are not properly intercepted. Therefore, much attention has been paid to avoiding these problems [38] by means of a more safe and robust formulation of the analytical solution. In the model SAILH, this robust formulation had not been implemented yet. This, however, has now been realized in the new model 4SAIL. Fig. 2 demonstrates how the increased robustness of 4SAIL has improved the numerical stability of the model compared to SAILH.

In this section, we describe the incorporation of thermal emission in four-stream canopy RT models. François [45] applied a similar approach with the SAIL model, calling it SAIL IRT, but here, we take the four-stream RT equations forming the basis of the SAIL model as a starting point, allowing also an extension to more complex cases with nonuniform leaf and soil temperatures and with non-Lambertian soil emissivity. In addition, Liu *et al.* [46] adapted a two-layer SAIL model to the TIR domain.

In the four-stream RT modeling concept (Fig. 1), we distinguish the following radiant fluxes:

1) direct solar irradiance (collimated flux density) on a horizontal plane E_s;
2) hemispherical diffuse downward irradiance E^-;
3) hemispherical diffuse upward irradiance E^+;
4) flux-equivalent radiance in the direction of observation E_o.

The term "flux-equivalent" radiance [42] is used because it designates the equivalent hemispherical flux that would result if the given surface radiance would be isotropic. Effectively, this definition implies the relation $E_o = \pi L_o$, where L_o is the radiance in the observer's direction.

Four-stream RT theory [42] describes the interactions among these four fluxes. For infinitesimal leaf layers, this leads to a system of four linear differential equations; for a thick but finite canopy layer, one obtains four ordinary linear equations, and for a background surface (e.g., the soil), two additional linear equations. The four-stream differential equations forming the basis of the SAIL models [38], [42] are given by

$$\begin{aligned}
\frac{d}{Ldx}E_s &= kE_s \\
\frac{d}{Ldx}E^- &= -s'E_s + aE^- - \sigma E^+ \\
\frac{d}{Ldx}E^+ &= sE_s + \sigma E^- - aE^+ \\
\frac{d}{Ldx}E_o &= wE_s + \nu E^- + \nu' E^+ - KE_o
\end{aligned} \tag{1}$$

where L is the LAI, x is the so-called relative optical height, which runs from -1 at the bottom to zero at the canopy top, and the coefficients are various extinction and scattering coefficients describing the interactions among the four flux types. They are dimensionless and depend only on the LIDF, the leaf optical properties, and the observational geometry [4]. The formal solution of (1) applied in order to enable the employment of the adding method [42] gives a set of relations between all fluxes incident to the layer and all reflected or transmitted fluxes. This set of relations is given by

$$\begin{aligned}
E_s(-1) &= \tau_{\rm ss}E_s(0) \\
E^-(-1) &= \tau_{\rm sd}E_s(0) + \tau_{\rm dd}E^-(0) + \rho_{\rm dd}E^+(-1) \\
E^+(0) &= \rho_{\rm sd}E_s(0) + \rho_{\rm dd}E^-(0) + \tau_{\rm dd}E^+(-1) \\
E_o(0) &= \rho_{\rm so}E_s(0) + \rho_{\rm do}E^-(0) + \tau_{\rm do}E^+(-1) + \tau_{\rm oo}E_o(-1)
\end{aligned} \tag{2}$$

where the ρ quantities indicate the reflectances, and the τ quantities indicate the transmittances of the isolated canopy layer. The double subscripts indicate the types of flux on incidence and exit, respectively, where s stands for solar, d for diffuse hemispherical, and o for flux in the observer's direction. This terminology [42] can be applied to describe the interactions between canopy and the soil background or the coupling of layers in a multilayered canopy. The various types of interaction [47] indicated by the double-subscript notation can be summarized by the following terms:

- so bidirectional (reflectance);
- ss direct (transmittance) in the direction of the solar beam;
- sd directional-hemispherical (for solar flux);
- dd bihemispherical;
- do hemispherical-directional (in viewing direction);
- oo direct (transmittance) in the direction of observation.

For a vegetation canopy, we can identify $\tau_{\rm oo}$ as the observed gap fraction, and one minus this quantity equals the observed cover fraction (OCF).

In order to incorporate thermal emission in this four-stream concept, we need to extend the associated differential equations of RT (1) with additional source terms due to thermal emission by leaves. Here, we assume that leaves emit thermal radiance isotropically and on both sides in equal amounts. For the simplest case of a uniform vegetation temperature T_ν, this gives

$$\begin{aligned}
\frac{d}{Ldx}E_s &= kE_s \\
\frac{d}{Ldx}E^- &= -s'E_s + aE^- - \sigma E^+ - \varepsilon_\nu H_\nu \\
\frac{d}{Ldx}E^+ &= sE_s + \sigma E^- - aE^+ + \varepsilon_\nu H_\nu \\
\frac{d}{Ldx}E_o &= wE_s + \nu E^- + \nu' E^+ - KE_o + K\varepsilon_\nu H_\nu
\end{aligned} \tag{3}$$

where ε_ν is the single-leaf emissivity. The hemispherical flux H_ν is the result of thermal emission by blackbody leaves at a temperature T_ν and is given by

$$H_\nu = \pi B(T_\nu)$$

where B is Planck's spectral radiance function for the indicated canopy temperature and the associated wavelength. We should emphasize that (3), in principle, apply to any monospectral radiation in the entire optical-thermal domain, although we realize that, in the TIR region, one can probably neglect the direct solar flux E_s, whereas in the solar-reflective regime, one could neglect the thermal emitted flux H_ν. We also note that the model does not turn into a process model by this extension, i.e., leaf temperatures are not modeled but are expected to be given as an input parameter.

The analytical solution of (3) can be expressed by means of an extended version of (2). The result is given by

$$\begin{aligned}
E_s(-1) &= \tau_{\rm ss}E_s(0) \\
E^-(-1) &= \tau_{\rm sd}E_s(0) + \tau_{\rm dd}E^-(0) + \rho_{\rm dd}E^+(-1) + \gamma_d H_\nu \\
E^+(0) &= \rho_{\rm sd}E_s(0) + \rho_{\rm dd}E^-(0) + \tau_{\rm dd}E^+(-1) + \gamma_d H_\nu \\
E_o(0) &= \rho_{\rm so}E_s(0) + \rho_{\rm do}E^-(0) + \tau_{\rm do}E^+(-1) \\
&\quad + \tau_{\rm oo}E_o(-1) + \gamma_o H_\nu.
\end{aligned} \tag{4}$$

Here, two new quantities have been introduced, which are given by

$$\begin{aligned}
\gamma_d &= 1 - \rho_{\rm dd} - \tau_{\rm dd} \\
\gamma_o &= 1 - \rho_{\rm do} - \tau_{\rm do} - \tau_{\rm oo}.
\end{aligned} \tag{5}$$

According to these definitions, they can be interpreted as absorptances, and because of Kirchhoff's Law, they can be identified as the hemispherical and the directional emissivity of the isolated canopy layer, respectively.

For a Lambertian soil, which is placed underneath the vegetation layer, one obtains the equation

$$E_o(-1) = E^+(-1) = r_s\left[E_s(-1) + E^-(-1)\right] + \varepsilon_s H_s \tag{6}$$

where r_s is the Lambertian soil reflectance, ε_s $(= 1 - r_s)$ is the soil emissivity, and the upward hemispherical thermal flux from the blackbody soil is given by $H_s = \pi B(T_s)$ for a soil temperature T_s. Combined with the second line of (4), this equation can be used to solve the fluxes at the soil level (bottom of canopy), after which, these can be inserted in the last line of (4) to solve the TOC flux-equivalent radiance. This finally gives

$$\begin{aligned}
E_o(0) = &\left[\rho_{\rm so} + \frac{(\tau_{\rm sd} + \tau_{\rm ss})r_s(\tau_{\rm do} + \tau_{\rm oo})}{1 - r_s\rho_{\rm dd}}\right]E_s(0) \\
&+ \left[\rho_{\rm do} + \frac{(\tau_{\rm do} + \tau_{\rm oo})r_s\tau_{\rm dd}}{1 - r_s\rho_{\rm dd}}\right]E^-(0) \\
&+ \left[\gamma_o + \frac{(\tau_{\rm do} + \tau_{\rm oo})r_s\gamma_d}{1 - r_s\rho_{\rm dd}}\right]H_\nu + \frac{(\tau_{\rm do} + \tau_{\rm oo})}{1 - r_s\rho_{\rm dd}}\varepsilon_s H_s.
\end{aligned} \tag{7}$$

The above expression is the unified solution for the entire optical-thermal spectral range which one obtains as a result of applying (3)–(6). It can be qualified as the simplest solution obtained for a Lambertian soil reflectance and a homogeneous turbid-medium canopy layer with uniform leaf temperature. Multiple scattering is included, however, and neglecting the direct solar flux gives a result similar to the one published by François [45], which can be expressed by

$$\pi L_o(0) = r_{\rm do}E^-(0) + \gamma_{\rm to}H_\nu + \tau_{\rm to}\varepsilon_s H_s \tag{8}$$

where

$$\begin{aligned}
r_{\rm do} &= \rho_{\rm do} + \tau_{\rm to}r_s\tau_{\rm dd} \\
\gamma_{\rm to} &= \gamma_o + \tau_{\rm to}r_s\gamma_d \\
\tau_{\rm to} &= \frac{\tau_{\rm do} + \tau_{\rm oo}}{1 - r_s\rho_{\rm dd}}.
\end{aligned} \tag{9}$$

We can identify the quantity $\gamma_{\rm to}$ (François [45] uses the symbol $\omega_{\rm to}$) as the effective vegetation directional emissivity and the quantity $\tau_{\rm to}\varepsilon_s$ as the effective soil emissivity of the ensemble [48]. Here, the effective emissivity is defined as the coefficient, applied to the radiance emitted by a certain component, to obtain the associate TOC radiance contribution. It can be shown that their sum $\gamma_{\rm to} + \tau_{\rm to}\varepsilon_s$ is equal to $1 - r_{\rm do}$, or one minus the associate hemispherical-directional reflectance, as should be expected for a physically consistent theory.

The four-stream reflectance and transmittance quantities of the isolated canopy layer appearing in (4) are all provided as regular output parameters of models like SAILH and 4SAIL already. This implies that, for simulations in the TIR, nothing special has to be added to these models to enable the calculation of directional emissivity and radiometric temperatures as long as leaf temperatures are uniform. One can show that this even holds true if the soil temperatures in the sun and in the shade would be different. Even in that case, one can apply the optical quantities given by these models on output, provided that one performs a "hotspot-effect" treatment, by applying the

bidirectional gap fraction to the soil's contribution, which is relatively simple. However, this does not hold any more if sunlit and shaded leaves have different temperatures as well. Therefore, we have carried out a dedicated analysis for this case.

The so-called optical hotspot effect is connected with the finite size of leaves in a canopy, as opposed to an infinitesimal size assumed in turbid-medium models. When the viewing direction is nearly along the sunrays, one obtains an enhanced reflectance due to the fact that, in this direction, almost no shadowed leaves and soil are observed but a majority of sunlit leaves and soil. This effect has been extensively described as well as modeled [38], [44], [49], so it does not have to be repeated here. In SAILH, the computation of the bidirectional canopy reflectance $\rho_{\rm so}$ has been modified to account for this finite leaf size, and an additional quantity called the bidirectional gap fraction, symbolized as $\tau_{\rm ssoo}$, has been added to the output parameters describing the canopy layer's optical properties.

This concludes the discussion of the optical origin of the hotspot effect. However, if sunlit leaves and soil are warmer than shaded leaves and soil because they receive more solar radiation, then these sunlit components are more likely to be viewed in the hotspot direction than in other directions. Thus, a hotspot effect can occur in the TIR spectral region as well, even when the solar irradiance in this wavelength region is negligible. We have analyzed this situation in detail, and the final result is an extended version of (4), which is given by

$$\begin{aligned} E_s(-1) &= \tau_{\rm ss}E_s(0) \\ E^-(-1) &= \tau_{\rm sd}E_s(0) + \tau_{\rm dd}E^-(0) + \rho_{\rm dd}E^+(-1) \\ &\quad + \gamma_d H_c + \gamma'_{\rm sd}\varepsilon_\nu(H_h - H_c) \\ E^+(0) &= \rho_{\rm sd}E_s(0) + \rho_{\rm dd}E^-(0) + \tau_{\rm dd}E^+(-1) \\ &\quad + \gamma_d H_c + \gamma_{\rm sd}\varepsilon_\nu(H_h - H_c) \\ E_o(0) &= \rho_{\rm so}E_s(0) + \rho_{\rm do}E^-(0) + \tau_{\rm do}E^+(-1) \\ &\quad + \tau_{\rm oo}E_o(-1) + \gamma_o H_c + \gamma_{\rm so}\varepsilon_\nu(H_h - H_c). \end{aligned} \quad (10)$$

Here, the hemispherical thermal fluxes associated with the blackbody hot leaves in the sun and cold leaves in the shade are supposed to be given by H_h and H_c, respectively. Three new coefficients have emerged from this analysis, namely, $\gamma_{\rm sd}$, $\gamma'_{\rm sd}$, and $\gamma_{\rm so}$. These coefficients have only an effect if there is a temperature difference between sunlit and shaded leaves. They are provided as output of the 4SAIL model. They are not computed by the SAILH model, so this model is only suitable for simulating cases with a uniform leaf temperature. We should emphasize that, although sunlit and shaded leaf temperatures were allowed to be different, it was assumed that these temperatures were constant with height. The average leaf temperature varies with depth in the canopy, but this is only because sunlit leaves become less frequent in the deeper canopy layers. The temperatures of both categories of leaves are still assumed constant. If this is known to be not the case, then one should apply (10) for a number of distinct canopy layers and employ a layer-adding algorithm in order to derive TOC radiance. However, this is left for future development whenever found necessary.

Another effect one can include in the unified four-stream approximation is that of a non-Lambertian soil reflectance and emissivity. Combined with the modeling of the optical and thermal hotspot effects, this gives the following unified expression for TOC flux-equivalent radiance:

$$\begin{aligned} E_o(0) &= \left[\rho_{\rm so} + \tau_{\rm ssoo}r_{\rm so} + \frac{(\tau_{\rm ss}r_{\rm sd} + \tau_{\rm sd}r_{\rm dd})\tau_{\rm do} + (\tau_{\rm sd} + \tau_{\rm ss}r_{\rm sd}\rho_{\rm dd})r_{\rm do}\tau_{\rm oo}}{1 - r_{\rm dd}\rho_{\rm dd}}\right] \\ &\quad \times E_s(0) + \left[\rho_{\rm do} + \frac{\tau_{\rm dd}(r_{\rm dd}\tau_{\rm do} + r_{\rm do}\tau_{\rm oo})}{1 - r_{\rm dd}\rho_{\rm dd}}\right] E^-(0) \\ &\quad + \left[\gamma_o + \frac{\gamma_d(r_{\rm dd}\tau_{\rm do} + r_{\rm do}\tau_{\rm oo})}{1 - r_{\rm dd}\rho_{\rm dd}}\right] H_c \\ &\quad + \left[\varepsilon_o\tau_{\rm oo} + \frac{\varepsilon_d(\tau_{\rm do} + \rho_{\rm dd}r_{\rm do}\tau_{\rm oo})}{1 - r_{\rm dd}\rho_{\rm dd}}\right] H_d \\ &\quad + \left[\gamma_{\rm so} + \frac{\gamma'_{\rm sd}(r_{\rm dd}\tau_{\rm do} + r_{\rm do}\tau_{\rm oo})}{1 - r_{\rm dd}\rho_{\rm dd}}\right] \varepsilon_\nu(H_h - H_c) \\ &\quad + \left[\varepsilon_o\tau_{\rm ssoo} + \frac{\tau_{\rm ss}\varepsilon_d(\tau_{\rm do} + \rho_{\rm dd}r_{\rm do}\tau_{\rm oo})}{1 - r_{\rm dd}\rho_{\rm dd}}\right] (H_s - H_d). \end{aligned} \quad (11)$$

In the above expression, the first two terms include the bidirectional reflectance of the ensemble, incorporating the optical hotspot effect and the directional reflectance for hemispherical diffuse incident radiation from the sky. The remaining four terms describe thermal emission associated with, respectively, cold leaves in the shade, soil in the shade, the temperature difference between hot and cold leaves, and the temperature difference between sunlit and shaded soil. The hotspot effect is incorporated in the quantities $\rho_{\rm so}$, $\tau_{\rm ssoo}$ (bidirectional gap fraction), and $\gamma_{\rm so}$. The soil's non-Lambertian reflection properties are expressed by the soil reflectance terms $r_{\rm so}$, $r_{\rm do}$, $r_{\rm sd}$, and $r_{\rm dd}$ (bidirectional, hemispherical-directional, directional-hemispherical, and bihemispherical reflectance, respectively). These can be calculated by applying, e.g., Hapke's soil BRDF model [50]. If, in (11), the soil is approximated by a Lambertian surface, one has to replace all four soil reflectances by one single reflectance r_s. The last term of (11) covers the case of sunlit parts of the soil having a different temperature than shaded parts, with the corresponding hemispherical thermal blackbody radiant fluxes indicated by H_s and H_d, respectively.

Without a thermal differentiation of sunlit and shaded foliage and soil, and by neglecting the solar incident flux in the thermal domain, only the second to fourth terms on the right-hand side of (11) are left, and one obtains the simplified expression

$$\pi L_o(0) = r^*_{\rm do}E^-(0) + \varepsilon^{\rm AEE}_\nu H_\nu + \varepsilon^{\rm AEE}_s H_s \quad (12)$$

where $\varepsilon^{\rm AEE}_\nu$ and $\varepsilon^{\rm AEE}_s$ are the so-called overall effective emissivities [48] of vegetation and the soil, respectively. The coefficients defined above can directly be taken from (11) and, thus, are given by

$$\begin{aligned} r^*_{\rm do} &= \rho_{\rm do} + \frac{\tau_{\rm dd}(r_{\rm dd}\tau_{\rm do} + r_{\rm do}\tau_{\rm oo})}{1 - r_{\rm dd}\rho_{\rm dd}} \\ \varepsilon^{\rm AEE}_\nu &= \gamma_o + \frac{\gamma_d(r_{\rm dd}\tau_{\rm do} + r_{\rm do}\tau_{\rm oo})}{1 - r_{\rm dd}\rho_{\rm dd}} \\ \varepsilon^{\rm AEE}_s &= \varepsilon_o\tau_{\rm oo} + \frac{\varepsilon_d(\tau_{\rm do} + \rho_{\rm dd}r_{\rm do}\tau_{\rm oo})}{1 - r_{\rm dd}\rho_{\rm dd}}. \end{aligned} \quad (13)$$

If one applies Kirchhoff's Law to the hemispherical and directional emissivities of the soil, i.e., applying the relationships $\varepsilon_d = 1 - r_{\mathrm{dd}}$ and $\varepsilon_o = 1 - r_{\mathrm{do}}$, it can be shown that the sum of the above three quantities equals unity. This forms an additional indication for the internal consistency of the followed approach.

III. Functioning of 4SAIL for the TIR and Comparison With Other Models and Measurements

The objective of this section is to investigate the performance of 4SAIL for TIR simulations. First, we describe the measured data obtained during two different campaigns, SPectra bARrax Campaign 2004 (SPARC2004) at Barrax, Spain, and Quantitative Remote Sensing: theory and application for Land Surface Parameters (QRSLSP) in Shunyi, China (2001). Some SPARC2004 data have been used as model inputs to study the general functioning of the model; the Shunyi data were used to compare simulated results with measurements and with those of other models.

A. Experimental Data Used for Model Evaluation

The first set of data consists of component-temperature measurements over a vineyard canopy during the SPARC2004 field campaign [54] in July 2004. The second dataset comprises measurements of canopy components and canopy directional brightness temperatures made over a winter wheat canopy in Shunyi, China, during the field experiment of the QRSLSP campaign [39] in April and May of 2001.

The experimental site of SPARC2004 was located in Barrax in the La Mancha region, Spain, in July of 2004. The site coordinates are 39.06° N and 2.10° W. The site was dominated by croplands, among which a small area of vineyard was planted. The rows of the vineyard were northwest–southeast oriented, with a canopy height of about 1.5 m, row spacing of 3.2 m (plant-stem to plant-stem), plant spacing of 1.6 m along the row direction, and plant spread width of 1.5 m across row direction. Leaves were clumped so that leaves in the lower location were overlaid by upper leaves and were completely in the shadow. The grape plants were irrigated by a drop-pipe system everyday. While soil surfaces near the pores of irrigation pipes located were wet, soil surfaces in between the rows were rather dry. In addition to many other measurements during the SPARC2004 field campaign, four thermal radiometers were set up on masts pointing to sunlit and shaded soil and sunlit and shaded leaves to take measurements of brightness temperatures of the four components on July 16, 2004. Table I gives an overview of the characteristics of the thermal radiometers used for canopy component-temperature measurements. The radiometers were calibrated both in the laboratory and in the field. LAI was measured with a LI-COR LAI 2000 instrument. Atmospheric radiosounding measurements were made at 08:07 UTC, 11:05 UTC, and 12:23 UTC, respectively, on July 16, 2004, to obtain atmospheric profiles of temperature and water vapor. These atmospheric profiles were applied in the MODTRAN4 model to calculate sky brightness temperatures. They varied from -16 °C to -12 °C. The local climate in Barrax on July 16, 2004, was clear, warm, and dry, with maximum air temperature of 30.6 °C, minimum relative humidity of 30%, and a maximum global radiation of 1054 W/m^2 at a reference height of 2.5 m.

TABLE I
Characteristics of Thermal Radiometers Used for Component Temperature Measurements in the SPARC2004 Field Experiment at Barrax, Spain

Radiometer model	Spectral range (μm)	Measurement range (° C)	Accuracy (° C)	FOV (°)	Target
Everest 3000	8 - 14	-30 to 100	0.2	25	sunlit leaves; shaded soil
Everest 4000	8 - 14	-30 to 100	0.2	15	shaded leaves; sunlit soil

TABLE II
Canopy Structure Parameters on April 11, 2001, and May 10, 2001, in the Two Winter Wheat Fields of the QRSLSP Experiment in Shunyi, China

Date	Site	species	LAI	Canopy height (cm)	Distance between row (cm)	Width of the wheat (cm)	Interval within wheat row (cm)
11 April	C3	9210	1.7	9.5	15	7	8
10 May	NW3	Jing 411	4.2	50	15	15	0

The QRSLSP site was located in the Shunyi county of Beijing in China from April to May in 2001. The Shunyi site was dominated by winter wheat in various varieties. Among other measurements, directional canopy brightness temperature was measured by thermal radiometers mounted on top of a goniometer. The goniometer was designed to make measurements of ground targets at different zenith view angles (maximum effective zenith angle up to 60°) and azimuth angles (between 0° and 360°) continuously according to desired angular intervals by preprogramming (see detailed description of goniometer measurements in [40] and [55]). Data were corrected to remove the temporal change in the measurements of brightness temperatures during a complete goniometer scan that was caused by variable meteorological conditions, i.e., solar radiation and wind speed. After such treatment, directionality in the measured canopy brightness temperature is mainly caused by the change of fractional cover of canopy components having different surface temperature in the field of view.

Measurements of component temperatures of sunlit and shaded leaves and of sunlit and shaded soil were made using a thermocouple thermometer (JM424 digital thermometer). The sensor of the JM424 digital thermometer is a K-type thermocouple (contact type) and has a nominal sensitivity of 0.1 K. The samplings were made simultaneously with goniometer measurements and randomly in the same wheat field but at different locations from those where directional canopy brightness temperature was measured by the goniometer.

The canopy structure was also measured during the entire experimental period and Table II gives the canopy parameters for the two days from which data were used in this paper as preliminary validation of the model.

Sky effective brightness temperature was measured using an AGA 80 radiometer following the method proposed by Chen and Zhang [56] in 1989.

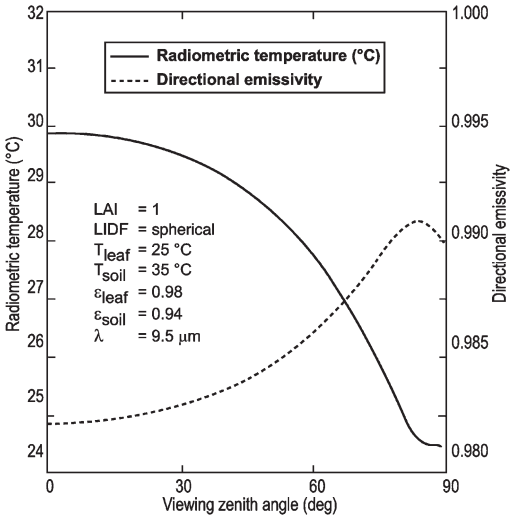

Fig. 3. Radiative temperature converted into degrees centigrade and (right scale) the directional emissivity as a function of the viewing zenith angle for the two-component case as computed with 4SAIL model. Legend: LAI = leaf area index; LIDF = leaf inclination distribution function; T leaf = temperature of the leaves; T soil = temperature of soil; ε leaf = emissivity of leaves; ε soil = emissivity of soil; λ = wavelength.

B. Simulation Results

As explained in Section II, it has been found that no modifications are needed to the SAIL models for their application to the TIR if the leaf temperature is uniform. At a given wavelength, on input, one only has to provide the emissivities and the kinetic temperatures of the leaves and the soil and the sky irradiance in the TIR. Under the assumption that leaves have zero transmittance in the TIR, one can call the model's subroutine for a single-leaf reflectance $\rho = 1 - \varepsilon_\nu$ and a soil reflectance $r_s = 1 - \varepsilon_s$, and next, the various optical output quantities of the canopy layer can be obtained. These are then used in a main program to compute TOC directional emissivity and TOC radiance, which can be converted into brightness temperature by inverting the Planck function for the associated wavelength. Here, the directional emissivity is always defined as one minus the hemispherical-directional reflectance at the same wavelength. Since, in this way, the directional emissivity of the ensemble is available, radiometric temperature can be computed by correcting the TOC radiance for the emissivity and downwelling atmospheric radiation. An example is shown in Fig. 3, which we obtained from the 4SAIL model. However, SAILH, or even the original SAIL model, would do just as well, since for modeling of canopy emissivity and TOC radiometric temperature under the given conditions the turbid-medium solution is already adequate, as the hotspot effect plays no role here. The model SAILH is the minimum required in order to take account of temperature differences between the sunlit and shaded soil fractions for uniform leaf temperatures, since in this case, a hotspot related in observing sunlit parts of the soil will emerge. Maximum flexibility, however, is offered by the new 4SAIL model, since with this model, sunlit and shaded leaves may have distinct temperatures as well.

Before the results obtained with the 4SAIL model are compared to those of other models and measurements, we first show some examples illustrating its behavior in relation to key parameters like the LAI, LIDF, fractional vegetation cover, and viewing direction for a wavelength of 9.5 μm. In order to clearly illustrate the model's behavior as a function of the sunlit and shaded leaf and soil temperatures, rather extreme cases have been taken as inputs. Yet, these cases originate from the real measurements from the SPARC2004 campaign on a hot and nearly windless day in July 2004 [51]. Under these extreme conditions, very large temperature differences were found (the total list of input parameters used as input for the simulations is presented in Table III). In all cases, four LAI values were taken (0.5, 1, 2, and 4), and four LIDFs, namely, planophile, plagiophile, spherical, and erectophile. These leaf-angle distributions are illustrated in cumulative form in Fig. 4. The hotspot parameter, approximately equal to the ratio leaf width/canopy height, is 0.05 in all simulated cases. The temperature differences are not meant to represent any real case, since the row-structured vineyard canopy is certainly not well represented by the homogeneous canopies simulated with this model, which probably would have less extreme temperature

TABLE III
INPUT VARIABLES FOR SIMULATIONS DEMONSTRATING MODEL BEHAVIOR

Variable	Simulation 1	Simulation 2
Local time	11:40	15:30
sza (deg)	37.5	24.2
Wavelength	9.5 μm	9.5 μm
LAI	0.5; 1; 2; 4	0.5; 1; 2; 4
Hot spot par.	0.05	0.05
Leaf emissivity	0.98	0.98
Soil emissivity	0.94	0.94
Th	37 C	42 C
Tc	29 C	33 C
Ts	50 C	58 C
Td	26 C	42 C
Tsky	-14 C	-14 C

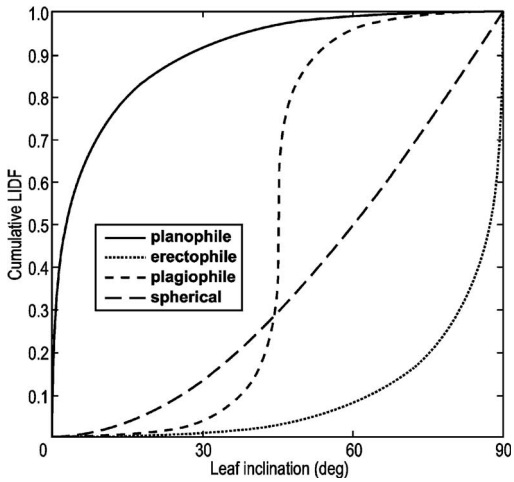

Fig. 4. Modeled cumulative LIDFs.

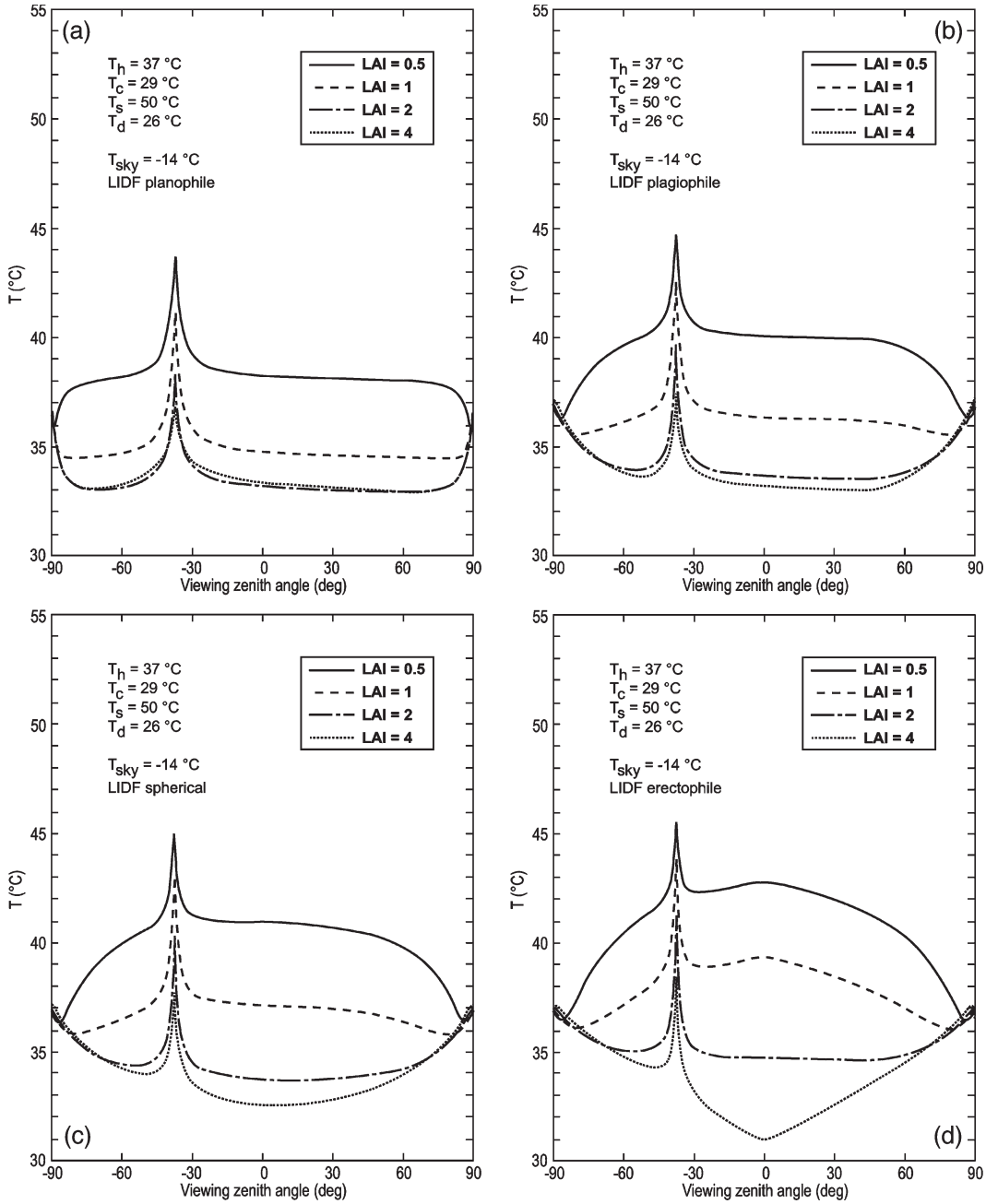

Fig. 5. Simulated directional brightness-temperature profiles in the principal plane for four LAI values and four LIDFs. (a) Planophile, (b) plagiophile, (c) spherical, and (d) erectophile. Temperatures for sunlit and shaded leaves and sunlit and shaded soil taken from Barrax measurements at 11:40 h local time. Sky radiative temperature is -14 °C.

differences. Nevertheless, it is interesting to observe how modeled directional brightness temperatures in the principal plane vary, showing a clear thermal hotspot and many features one can often observe in the optical domain as well. The results are plotted in Figs. 5 and 6, which represent two moments of day, at 11:40 and 15:30 h local time, respectively. The longwave downward diffuse flux was also measured, and it has been converted into a sky brightness temperature in degrees centigrade, since the application program requires this on input. It was found, by the way, that totally neglecting the longwave radiation flux from the sky gives only a 0.3 °C lower brightness temperature on output. Because of the small effect of this parameter, for both situations, a narrowband sky brightness temperature of -14 °C was taken. From Figs. 5 and 6, one may conclude that directional signatures of brightness temperature depend strongly on the LIDF but also on the LAI and the component temperatures. The hotspot peak is related to temperature differences between sunlit and shaded foliage and soil, and it is difficult to separate both influences. One may expect that, at high LAI, it will be more related to the foliage and, at low LAI, more to the soil, but this is only partly confirmed in the plots. Additional simulations, in which there is only a sunlit–shaded temperature difference for either the foliage or the soil but not both, would be necessary in order to

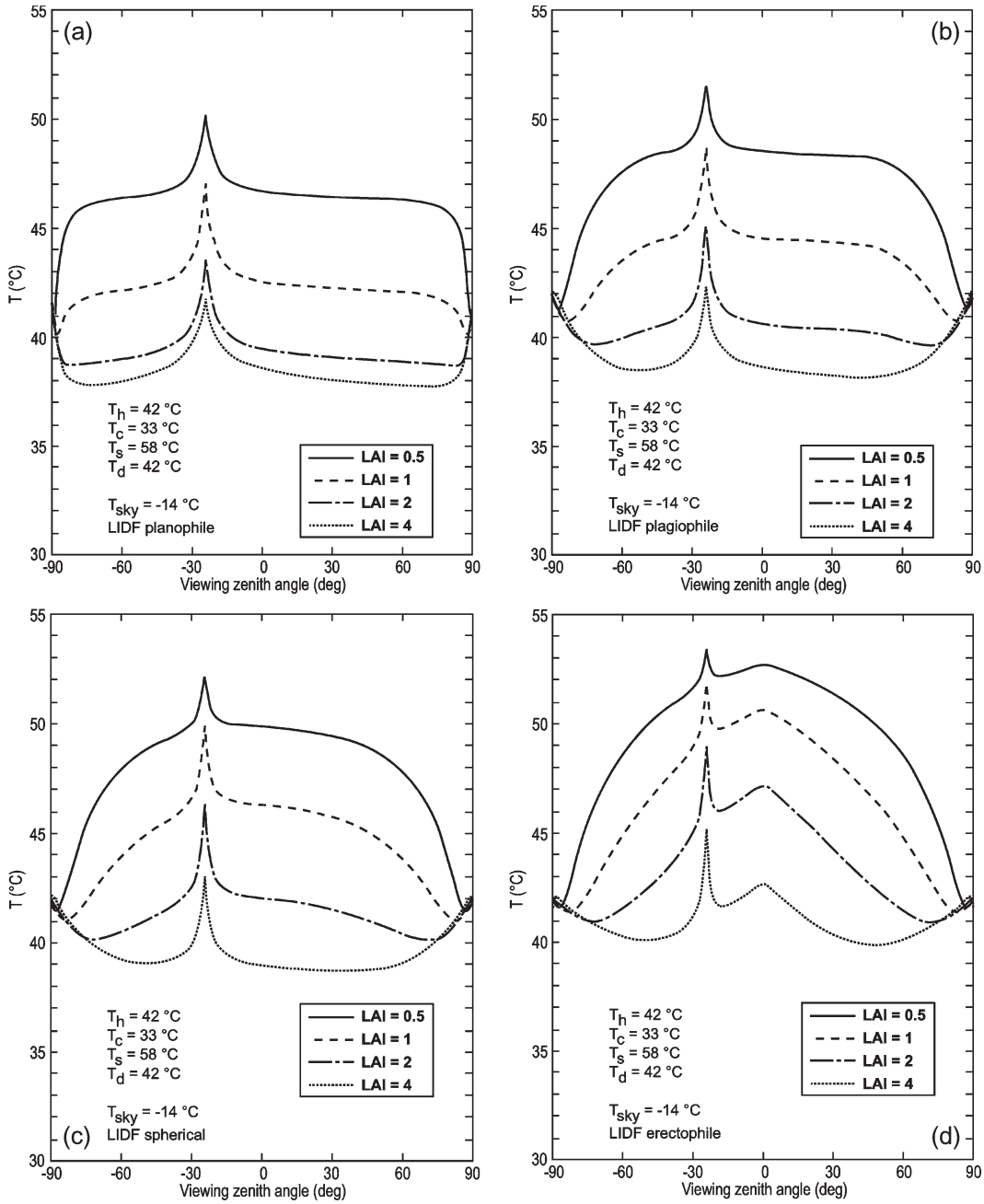

Fig. 6. As Fig. 5, but for Barrax temperature measurements at 15:30 h local time.

investigate this issue in some more detail. In addition, it is not immediately clear how multiple-view-angle (MVA) thermal-radiance observations would allow one to retrieve separate component temperatures from them if no other information is given. However, combined with optical MVA observations, one might be able to apply model inversion techniques to both types of data simultaneously, thus enabling the retrieval of canopy structure along with component temperatures. The simulations also demonstrate that, for canopies as discussed here, with significant temperature differences between sunlit and shaded components, the two-component linear-mixture model appears to be an oversimplification, since directional signatures of brightness temperature are strongly influenced by temperature differences between the sunlit and shaded components.

In order to investigate the TOC directional emissivities for the same situations as displayed in Figs. 5 and 6, we have plotted these as a function of the viewing zenith angle in Fig. 7 and as a function of the OCF in Fig. 8. From these plots, one can observe that emissivity always increases with LAI but in a nonlinear way. As a function of the viewing angle, the profile is strongly influenced by the LIDF. Because more vegetation is observed, a larger viewing angle gives mostly a higher emissivity, but for high LAI, the reverse can be true. The highest emissivity is found under nadir viewing, an LAI of four and an erectophile LIDF. In this case, the so-called cavity effect is higher than in the other cases. From Fig. 8, one may conclude that, for low LAI, the relation between emissivity and observed cover is linear and almost independent of the LIDF.

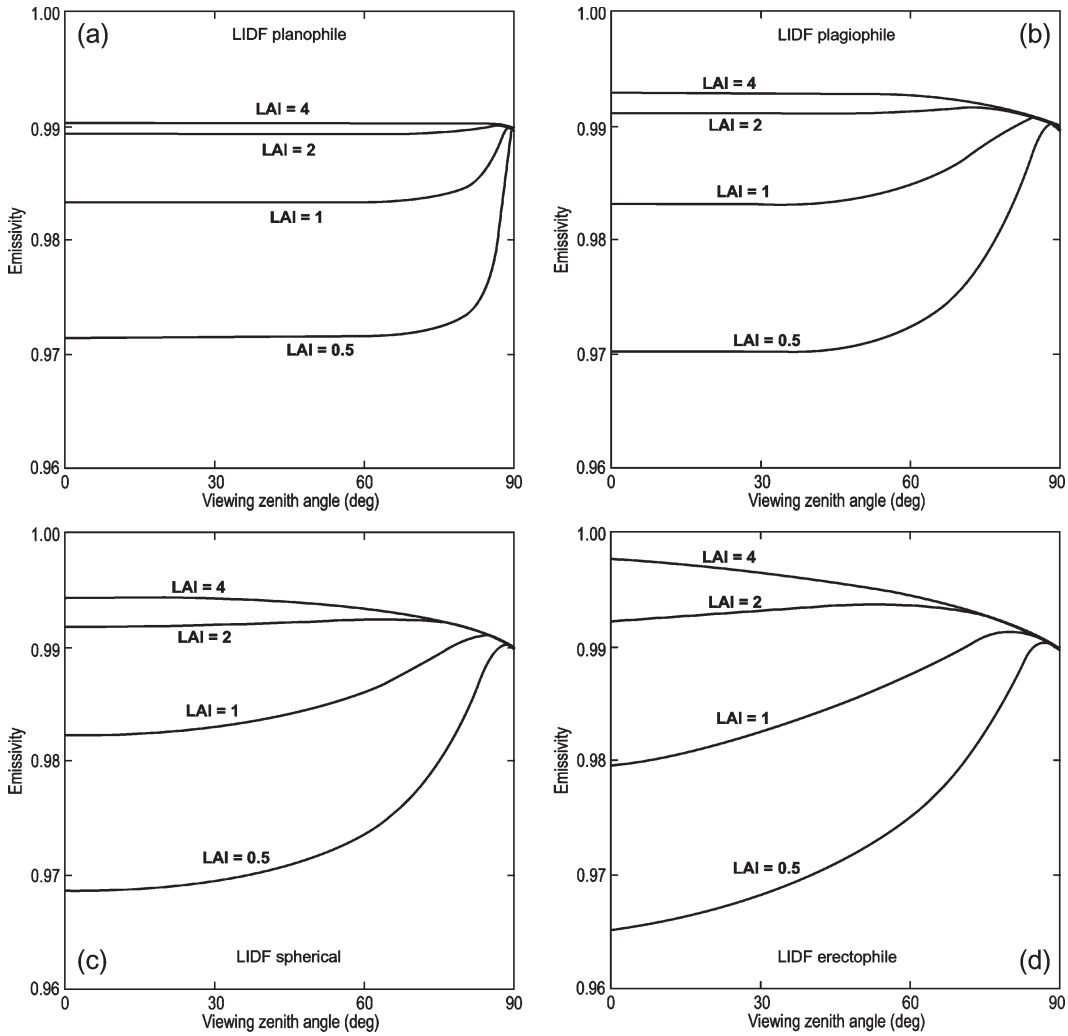

Fig. 7. Directional emissivity as a function of the viewing zenith angle for four LAI values and four LIDFs. (a) Planophile, (b) plagiophile, (c) spherical, and (d) erectophile.

However, this relationship still depends strongly on the LAI and becomes less linear and more dependent on the LIDF at higher LAI values. At an LAI of two, the relationship with observed cover is almost flat, with emissivities of about 0.99. For LAI $= 4$, the emissivity decreases with observed cover due to the decreasing cavity effect when the viewing direction approaches the horizon.

In what follows, we compare the performance of the 4SAIL model to those of other models for the two-component case and to measurements for the three- and four-component cases. In [45] and [52], a model called SAIL IRT was discussed. We have verified, both theoretically and numerically, that this model is equivalent to the two-component TIR version of SAILH, or SAIL, as hotspot effects are ignored in SAIL IRT, so comparisons with this model have been omitted here. Two other models are MOD3 and MOD4 in the study in [45]. Basically, MOD3 and MOD4 are two-component TIR RT models. MOD3 uses the directional gap frequency function to parameterize the multiple reflections between soil and canopy, but no additional cavity effect is included due to the assumed solid nature of the vegetation. MOD4 introduced an additional coefficient named "cavity-effect coefficient" to take into account the 3-D multiple scattering inside a vegetation canopy.

The simulation results of MOD3 and MOD4 were computed using the same input parameters as for 4SAIL, and a spherical leaf-angle distribution was assumed in all cases. The measured directional brightness temperatures and all other parameters were obtained from the experimental data collected over a winter wheat crop in the Shunyi remote sensing field campaign in China in 2001 [39], described earlier in this section. Table IV summarizes the most important model variables on both dates. The solar positions are given by the solar zenith angle sza and the solar azimuth angle saz. The selected measurements were taken perpendicularly to the row direction in order to reduce extreme row effects. Brightness temperature variations predicted by each model as a function of the view angle for two cases (Field C3, 12:30 h, April 11, 2001, LAI $= 1.7$ and Field NW3, 12:00 h, May 10, 2001, LAI $= 4.2$, respectively) are presented in Fig. 9.

The simulation results from MOD3, MOD4 presented in [45], and 4SAIL with two components are quite close to one another. In these cases, the mean temperatures of components

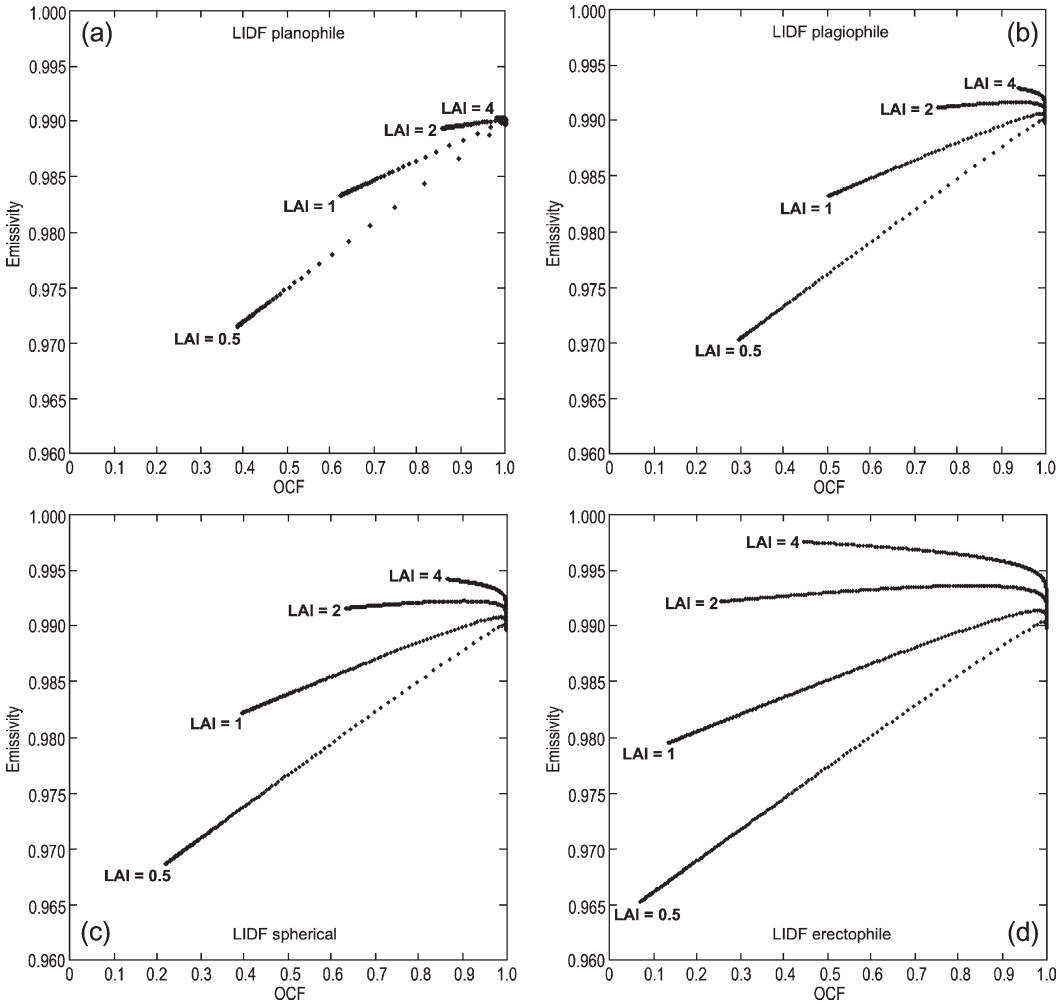

Fig. 8. Directional emissivity as a function of OCF for four LAI values and four LIDFs. (a) Planophile, (b) plagiophile, (c) spherical, and (d) erectophile.

TABLE IV
INPUT VARIABLES FOR SIMULATION OF MEASUREMENTS ON THE GIVEN DATES. DATA WERE COLLECTED OVER WINTER WHEAT CROP DURING THE SHUNYI FIELD CAMPAIGN IN CHINA FOR TWO DAYS IN 2001

Variable	11 April 2001	10 May 2001
Local time	12:30	12:00
sza (deg)	32.4	23.2
saz (deg)	187.2	174.4
LAI	1.7	4.2
Th (C)	21.3	24.2
Tc (C)	20.5	23.0
Ts (C)	25.2	25.8
Td (C)	19.9	23.1
Tsky (C)	-33.0	-31.0
ε_v	0.98	0.98
ε_s	0.96	0.96

in the sun and in the shade were taken as model inputs. The directional signatures are similar in shape, and it turns out that 4SAIL produces brightness temperatures that are consistently about 0.1 °C higher than those of MOD4 and about half a degree higher than those of MOD3. The spherical leaf-angle distribution is not the one that gives the best fit to the measurements, but because of the relatively strong row structure in the measured canopy, no attempts have been made to improve the fit by adjusting the leaf-angle distribution parameters. In the measurements of May 10, a hotspot effect is clearly visible [Fig. 9(c)]. This cannot be simulated by two-component models, but the overall flat signature is fairly well reproduced by all models.

Additional simulations have been carried out with 4SAIL for three- and four-component cases. It is illustrated [Fig. 9(b) and (d)] that these can simulate the hotspot feature quite well, and the simulations are also fairly close to the observed directional brightness temperatures for both cases, with differences not bigger than 0.5 K at large zenith angles. On April 11, the model simulations show a less good match with the measurements, which are not symmetric with respect to nadir and show a sharp decrease at larger zenith view angles, probably because of row effects, which are not included in either of the models. The result for May 10 shows that 4SAIL with four components gives a good match with the measurements. From these comparisons, we may conclude that 4SAIL with three and four components certainly has an advantage over

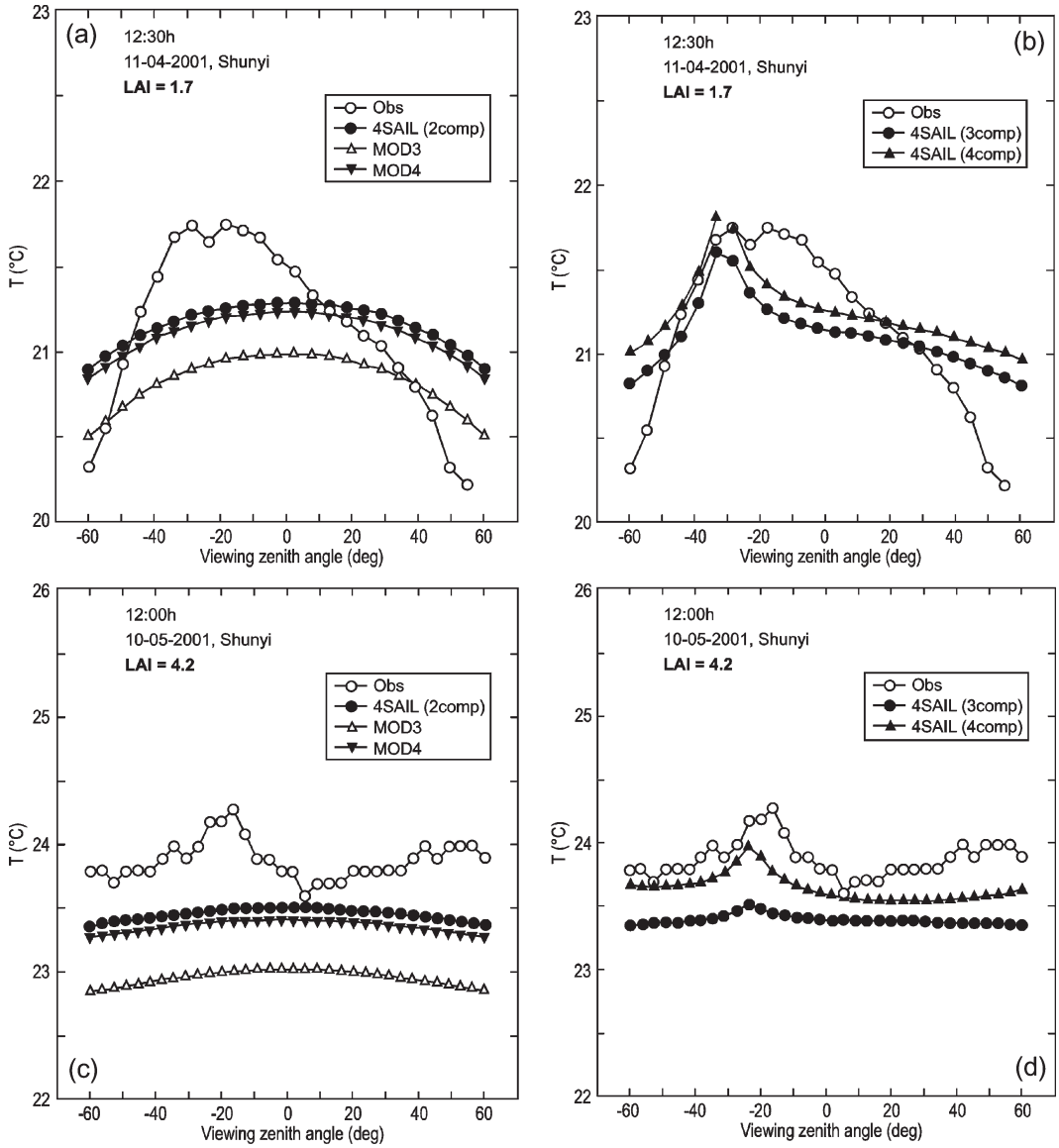

Fig. 9. Directional signatures of brightness temperature (in degrees centigrade) computed by 4SAIL compared with other models and with measurements: (a) April 11, 4SAIL (two component), MOD3, MOD4 versus measurements, (b) April 11, 4SAIL (three component), 4SAIL (four component) versus measurements, (c) May 10, 4SAIL (two component), MOD3, MOD4 versus measurements, and (d) May 10, 4SAIL (three component), 4SAIL (four component) versus measurements.

two-component models, because the hotspot effect can be simulated.

According to the study in [45], MOD4 performs nearly the same as the model of [53], which is a turbid-medium RT model in the case of homogeneous canopies, hence, the comparison presented here can also be considered valid for the homogeneous mode of [53].

Another work [35] has reported an extension of the DART model [15] to the TIR domain. Originally, DART was developed for the optical domain for simulating the RT within complex 3-D vegetation covers with a ray-tracing approach combined with a discrete-ordinate method.

A first validation of the extended DART was made using directional radiometric measurements from a cotton row crop collected in the early 1980s as presented in [24], in which, in addition to data on canopy geometry, radiometric data were collected on four scene components: sunlit and shaded vegetation and sunlit and shaded soil. Since the difference observed between the sunlit and shaded vegetation was less than 0.5 K for all sun-illumination conditions in the dataset [35], the vegetation temperature was set equal to the average measured one within the canopy. Using measured and prescribed parameters (when the measured ones were lacking because DART requires many parameters), they reported a root-mean-square (rms) deviation of 1.25 K between the simulated and measured radiometric temperatures for all solar and viewing directions in the dataset. By comparison, Kimes and Kirchner [19] validated their geometric projection model specifically designed for row crops and found an rms deviation of 0.96 K using the same dataset. The higher rms value obtained with the DART model was explained by the fact that some parameters required by the model were not collected

and instead assumed values were used, but for the geometric model, only the canopy geometry and the radiometric temperature of each cover component were required. A simulation of the hotspot feature by DART was not reported. Interestingly, Guillevic *et al.* [35] also tested their model against the model of [53] and found that the two models give very similar results.

From the above discussions, it appears legitimate for us to conclude that 4SAIL performs satisfactorily, judging from its analytical characteristics and its low demands in model inputs and computing power.

IV. Discussion

Simulations of the directionality of the brightness temperature and emissivity for soil–vegetation objects in the TIR have often been carried out with GO linear-mixture type of models. These models explain the directionality mainly by the change of observed vegetation cover fraction as a function of the viewing angle, in connection with the object's 3-D structure. However, in this paper, we have just demonstrated by means of a RT approach that, also for homogeneous vegetation canopies, the anisotropy in TIR observations can be considerable. In this case, the anisotropy should in the first place be attributed to changes of the observed fractional vegetation cover related to the LAI and the LIDF rather than to observed projections of 3-D objects like tree crowns or crop rows. For heterogeneous vegetation, GORT models combine both types of influences on vegetative cover, so these are expected to yield the most promising solutions to accurately modeling the anisotropy of TIR radiances.

Up to now, there has not been that much attention for temperature differences between sunlit and shaded foliage and soil. However, the simulations presented in the previous section suggest that actually measured leaf and soil temperature differences can lead to simulated thermal hotspot peaks of up to about 4° in height. Ignoring these effects might lead to serious errors in the interpretation of TIR observations. There is major theoretical evidence [see (10)] suggesting that sunlit–shaded foliage temperature differences do have a direct impact on the net longwave flux at TOC level as well, so this issue definitely deserves more attention in follow-on investigations.

The directional profiles of simulated brightness temperature shown in Figs. 5 and 6 have some resemblance to profiles of the bidirectional reflectance in the optical domain. For example, in the principal plane, a similar hotspot peak phenomenon can be observed. However, there are also differences: without the hotspot, the directional signature in the thermal domain would have been azimuthally symmetric, whereas in the optical domain, this would only be the case if the solar incident flux were absent, under an overcast sky for instance. This means that optical and thermal domain MVA observations provide partly complementary information and, thus, could be used in advanced retrieval algorithms to obtain more accurate information about canopy structure as well as more accurate component temperatures. In this respect, the former candidate ESA mission SPECTRA was clearly ahead of its time by its advanced instrumental design aimed at coregistered MVA (seven along-track viewing angles) hyperspectral thermal observations of the land surface.

V. Conclusion

In this paper, we extended four-stream RT theory to the TIR region so that the temperature differences between sunlit and shaded soil and sunlit and shaded leaves can be related to TOC radiance directionality. The modernized analytical four-stream RT model that is called 4SAIL enables us to directly simulate the scattering and emission of TIR radiation inside a geometrically homogeneous but thermodynamically heterogeneous canopy. This development may be considered as an important step towards the quantitative description that is urgently needed to address the relationship between the TIR directionality and component temperatures, which can be particularly important for sparsely vegetated areas where the soil and vegetation component temperatures in the sunlit and shaded areas may be very different depending on the solar radiation, physical state of the surface, and meteorological conditions.

Simulation results obtained with the model indicate that, for canopies with significant temperature differences between sunlit and shaded components, the two-component linear-mixture model appears to be an oversimplification, since directional signatures of brightness temperature are strongly influenced by temperature differences between the sunlit and shaded components.

The results also show that one cannot apply a simple, single emissivity and temperature model to structured vegetated land surfaces to invert infrared radiance measurements.

The advantage of using a single model for the whole spectral domain from visible to TIR is that the possible synergies between both spectral windows can be exploited better, since a common description of canopy architecture is used.

A detailed validation of the 4SAIL model, using experimental data collected for a winter wheat canopy during the Shunyi experiment in China in 2001, will be addressed in a future publication.

Acknowledgment

The authors would like to thank C. François for providing the models used in the comparison. They would also like to thank several anonymous reviewers for their valuable suggestions and comments.

References

[1] N. S. Goel, "Models of vegetation canopy reflectance and their use in estimation of biophysical parameters from reflectance data," *Remote Sens. Rev.*, vol. 4, pp. 1–212, 1988.

[2] B. Pinty, N. Gobron, J.-L. Widlowski, S. A. W. Gerstl, M. M. Verstraete, M. Antunes, C. Bacour, F. Gascon, J.-P. Gastellu, N. Goel, S. Jacquemoud, P. North, W. Qin, and R. Thompson, "The RAdiation Model Intercomparison (RAMI) exercise," *J. Geophys. Res.*, vol. 106, no. D11, pp. 11 937–11 956, 2001.

[3] G. H. Suits, "The calculation of the directional reflectance of a vegetative canopy," *Remote Sens. Environ.*, vol. 2, pp. 117–125, 1972.

[4] W. Verhoef, "Light scattering by leaf layers with application to canopy reflectance modeling: The SAIL model," *Remote Sens. Environ.*, vol. 16, no. 2, pp. 125–141, Oct. 1984.

[5] Y. V. Knyazikhin, A. L. Marshak, and R. B. Myneni, "Interaction of photons in a canopy of finite-dimensional leaves," *Remote Sens. Environ.*, vol. 39, no. 1, pp. 61–74, Jan. 1992.

[6] N. Gobron, B. Pinty, M. M. Verstraete, and Y. Govaerts, "A semi-discrete model for the scattering of light by vegetation," *J. Geophys. Res.*, vol. 102, no. D8, pp. 9431–9446, 1997.

[7] S. A. W. Gerstl and C. C. Borel, "Principles of the radiosity method versus radiative transfer for canopy reflectance modeling," *IEEE Trans. Geosci. Remote Sens.*, vol. 30, no. 2, pp. 271–275, Mar. 1992.

[8] M. Chelle, "Développement D'un Modèle De Radiosité Mixte Pour Simuler La Distribution du Rayonnement Dans Les Couverts Végétaux," Ph.D. thesis, Université de Rennes, Rennes, France, 1997.

[9] P. R. J. North, "Three-dimensional forest light interaction model using a Monte Carlo method," *IEEE Trans. Geosci. Remote Sens.*, vol. 34, no. 4, pp. 946–956, Jul. 1996.

[10] R. B. Myneni, G. Asrar, and E. T. Kanemasu, "Light scattering in plant canopies: The method of successive orders of scattering approximations (SOSA)," *Agric. For. Meteorol.*, vol. 39, no. 1, pp. 1–12, 1987.

[11] X. Li and A. H. Strahler, "Geometric-optical bidirectional reflectance modeling of a coniferous forest canopy," *IEEE Trans. Geosci. Remote Sens.*, vol. GRS-24, no. 6, pp. 906–919, 1986.

[12] X. Li and A. H. Strahler, "Geometric-optical bidirectional reflectance modeling of the discrete-crown vegetation canopy: Effect of crown shape and mutual shadowing," *IEEE Trans. Geosci. Remote Sens.*, vol. 30, no. 2, pp. 276–292, Mar. 1992.

[13] J. M. Norman and J. M. Welles, "Radiative transfer in an array of canopies," *Agron. J.*, vol. 75, pp. 481–488, 1983.

[14] X. Li, A. H. Strahler, and C. E. Woodcock, "A hybrid geometric optical radiative transfer approach for modeling albedo and directional reflectance of discontinuous canopies," *IEEE Trans. Geosci. Remote Sens.*, vol. 33, no. 2, pp. 466–480, Mar. 1995.

[15] J. P. Gastellu-Etchegory, V. Demarez, V. Pinel, and F. Zagolski, "Modeling radiative transfer in heterogeneous 3-D vegetation canopies," *Remote Sens. Environ.*, vol. 58, no. 2, pp. 131–156, Nov. 1996.

[16] H. Rahman, B. Pinty, and M. M. Verstraete, "Coupled surface-atmosphere reflectance (CSAR) model 2. Semi empirical surface model useable with NOAA advanced very high resolution radiometer data," *J. Geophys. Res.*, vol. 98, no. D11, pp. 20 791–20 801, 1993.

[17] J.-L. Roujean, M. Leroy, and P. Y. Deschamps, "A bidirectional reflectance model of the earth's surface for the correction of remote sensing data," *J. Geophys. Res.*, vol. 97, no. D18, pp. 20 455–20 468, 1992.

[18] W. Wanner, X. Li, and A. H. Strahler, "On the derivation of kernels for kernel-driven models of bidirectional reflectance," *J. Geophys. Res.*, vol. 100, no. D10, pp. 21 077–21 090, 1995.

[19] D. S. Kimes and J. A. Kirchner, "Directional radiometric measurements of row-crop temperatures," *Int. J. Remote Sens.*, vol. 4, no. 2, pp. 299–311, 1983.

[20] D. S. Kimes, "Remote sensing of row crop structure and component temperatures using directional radiometric temperatures and inversion techniques," *Remote Sens. Environ.*, vol. 3, no. 1, pp. 33–55, Mar. 1983.

[21] J. A. Sobrino and V. Caselles, "Thermal Infrared radiance model for interpreting the directional radiometric temperature of a vegetative surface," *Remote Sens. Environ.*, vol. 33, no. 3, pp. 193–199, Sep. 1990.

[22] J. A. Sobrino, V. Caselles, and F. Becker, "Significance of the remotely sensed thermal infrared measurements obtained over a citrus orchard," *ISPRS J. Photogramm. Remote Sens.*, vol. 44, pp. 343–354, 1990.

[23] V. Caselles, J. A. Sobrino, and C. Coll, "A physical model for interpreting the land surface temperature obtained by remote sensors over incomplete canopies," *Remote Sens. Environ.*, vol. 39, no. 3, pp. 203–211, Mar. 1992.

[24] D. S. Kimes, "Remote sensing of temperature profiles in vegetation canopies using multiple view angles and inversion techniques," *IEEE Trans. Geosci. Remote Sens.*, vol. 19, no. 2, pp. 85–90, GRS-1981.

[25] D. S. Kimes, J. A. Smith, and L. E. Link, "Thermal IR exitance model of a plant canopy," *Appl. Opt.*, vol. 20, no. 4, pp. 623–632, 1981.

[26] M. J. McGuire, J. A. Smith, L. K. Balick, and B. A. Hutchison, "Modeling directional thermal radiance from a forest canopy," *Remote Sens. Environ.*, vol. 27, no. 2, pp. 169–186, Feb. 1989.

[27] J. M. Norman and J. L. Chen, "Thermal emissivity and infrared temperatures dependence on plant canopy architecture and view angle," in *Proc. IGARSS*, 1990, pp. 1747–1750.

[28] J. A. Smith and S. M. Goltz, "A thermal exitance and energy balance model for forest canopies," *IEEE Trans. Geosci. Remote Sens.*, vol. 32, no. 5, pp. 1060–1066, Sep. 1995.

[29] J. Otterman, T. W. Brakke, and J. Susskind, "A model for inferring canopy and underlying soil temperatures from multi-directional measurements," *Boundary-Layer Meteorol.*, vol. 61, no. 1, pp. 81–97, Oct. 1992.

[30] J. Otterman, T. W. Brakke, M. Fuchs, V. Lakshmi, and M. Cadeddu, "Longwave emission from a plant/soil surface as a function of the view direction. Dependence on the canopy architecture," *Int. J. Remote Sens.*, vol. 20, no. 11, pp. 2195–2201, Jul. 1999.

[31] Z. Niu, Q. Liu, Y. Gao *et al.*, "The gap probability model for canopy thermal infrared emission with non-scattering approximation," *Sci. China, Ser. E* vol. 43, pp.83–94, 2000. (Suppl.)

[32] L. Chen, J. Zhuang, Q. Liu, X. Xu, and G. Tian, "Study on the law of radiant directionality of row crops," *Sci. China, Ser. E*, vol. 43, pp. 70–82, 2000. (Suppl.).

[33] G. Yan, L. Jiang, J. Wang, L. Chen, and X. Li, "Thermal bidirectional gap probability model for row crops and validation," *Sci. China, Ser. D, Earth Sci.*, vol. 46, no. 12, pp. 1241–1249, 2003.

[34] T. Yu, X. Gu, G. Tian, M. Legrand, F. Baret, J.-F. Hanocq, R. Bosseno, and Y. Zhang, "Modeling directional brightness temperature over a maize canopy in row structure," *IEEE Trans. Geosci. Remote Sens.*, vol. 42, no. 10, pp. 2290–2304, Oct. 2004.

[35] P. Guillevic, J.P. Gastellu-Etchegory, J. Demarty, and L. Prévot, "Thermal infrared radiative transfer within three-dimensional vegetation covers," *J. Geophys. Res.*, vol. 108, no. D8, pp. ACL6.1–ACL6.13, 2003. DOI: 10.1029/2002JD002247.

[36] W. C. Snyder and Z. Wan, "BRDF models to predict spectral reflectance and emissivity in the thermal infrared," *IEEE Trans. Geosci. Remote Sens.*, vol. 36, no. 1, pp. 214–225, Jan. 1998.

[37] X. Li, A. H. Strahler, and M. A. Friedl, "A conceptual model for effective directional emissivity from non-isothermal surfaces," *IEEE Trans. Geosci. Remote Sens.*, vol. 37, no. 5, pp. 2508–2517, Sep. 1999.

[38] W. Verhoef, "Theory of radiative transfer models applied in optical remote sensing of vegetation canopies," Ph.D. dissertation, Wageningen Agricultural Univ., Wageningen, The Netherlands, 1998.

[39] Q.-H. Liu, X. Li, and L.-F. Chen, "Field campaign for quantitative remote sensing in Beijing," in *Proc. IGARSS Symp.*, Toronto, ON, Canada, Jun. 24–28, 2002, vol. VI, pp. 3133–3135.

[40] L. Jia, "Modeling heat exchanges at the land-atmosphere interface using multi-angular thermal infrared measurements," Ph.D. dissertation, Wageningen Univ., Wageningen, The Netherlands, 2004.

[41] W. Verhoef and N. J. J. Bunnik, "Influence of crop geometry on multispectral reflectance determined by the use of canopy reflectance models," *Proc. Int. Colloq.* "*Spectral Signatures Objects Remote Sens.*," Avignon, France, Sep. 1981, pp. 273–290.

[42] W. Verhoef, "Earth observation modeling based on layer scattering matrices," *Remote Sens. Environ.*, vol. 17, no. 2, pp. 165–178, Apr. 1985.

[43] H. C. van de Hulst, *Multiple Light Scattering*. London, U.K.: Academic, 1980.

[44] A. Kuusk, "The hot spot effect of a uniform vegetative cover," *Sov. J. Remote Sens.*, vol. 3, no. 4, pp. 645–658, 1985.

[45] C. François, "The potential of directional temperatures for monitoring soil and leaf temperature and soil moisture status," *Remote Sens. Environ.*, vol. 80, no. 1, pp. 122–133, Apr. 2002.

[46] Q. Liu, L. Chen, Q. Liu, and Q. Xiao, "A radiation transfer model to predict canopy radiation in thermal infrared band," *J. Remote Sens.*, vol. 7, no. 3, pp. 161–167, 2002. (in Chinese).

[47] F. E. Nicodemus, "Reflectance nomenclature and directional reflectance and emissivity," *Appl. Opt.*, vol. 31, no. 36, pp. 7669–7683, Jun. 1970.

[48] L. F. Chen, Z.-L. Li, Q. H. Liu, S. Chen, Y. Tang, and B. Zhong, "Definition of component effective emissivity for heterogeneous and non-isothermal surfaces and its approximate calculation," *Int. J. Remote Sens.*, vol. 25, no. 1, pp. 231–244, Jan. 2004.

[49] F.-M. Bréon, F. Maignan, M. Leroy, and I. Grant, "Analysis of hot spot directional signatures measured from space," *J. Geophys. Res.*, vol. 107, no. D16, p. AAC1-1, 2002. DOI:10.1029/2001JD001094.

[50] B. W. Hapke, "Bidirectional reflectance spectroscopy 1. Theory," *J. Geophys. Res.*, vol. 86, pp. 3039–3054, 1981.

[51] Z. Su, L. Jia, A. Gieske, W. Timmermans, X. Jin, J. Elbers, H. van der Kwast, A. Olioso, J. A. Sobrino, F. Nerry, D. Sabol, and J. Moreno, "In-situ measurements of land-atmosphere exchanges of water, energy and carbon dioxide in space and time over the heterogeneous BARRAX site during SPARC2004," in *Proc. ESA WPP-250, SPARC Final Workshop, ITC Enschede*, The Netherlands, Jul. 4–5, 2005, pp. 1–8.

[52] A. Olioso, "Simulation des échanges d'énergie et de masse d'un couvert végétal, dans le but de relier la transpiration et la photosynthèse aux mesures de réflectance et de température de surface," Ph.D. dissertation, Université Montpellier II, Montpellier, France, 1992.

[53] L. Prévot, "Modélisation des échanges radiatifs au sein des couverts végétaux. Application à la télédétection. Validation sur un couvert de maïs," Doctoral Thesis, Univ. Paris VI, Paris, France, 1985.

[54] *SPARC 2004—SPARC Data Acquisition Report*, p. 199, Feb. 2005. ESA Contract 18307/04/NL/FF.
[55] Q. Liu, "Study on component temperature inversion algorithm and the scale structure for remote sensing pixel," Ph.D. dissertation, Inst. Remote Sens. Appl., Chinese Academy Sci., Beijing, China, 2002. (in Chinese with English abstract).
[56] J. M. Chen and R. H. Zhang, "Studies on the measurements of crop emissivity and sky temperature," *Agric. For. Meteorol.*, vol. 49, no. 1, pp. 23–34, 1989.

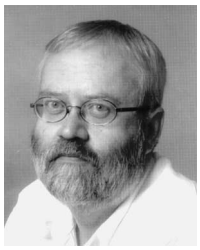

Wout Verhoef was born in Sliedrecht, The Netherlands, in 1951. He received the Ing. degree in physics engineering from the Technical College of Dordrecht, Dordrecht, The Netherlands, in 1972, and the Ph.D. degree in agricultural and environmental sciences from Wageningen University, Wageningen, The Netherlands, in 1998, through his continued work on radiative transfer modeling in vegetation canopies and the atmosphere.

He started his career in optical remote sensing at the Netherlands Interdepartmental Working community for the Application of Remote Sensing techniques (NIWARS), Delft, The Netherlands, where he was involved in a field spectrometer measurement program on vegetation, soils, and water. In 1977 he joined the National Aerospace Laboratory (NLR), The Netherlands, where he developed the widely known SAIL canopy reflectance model in 1981 and a range of improved variants. At NLR, he also developed image processing methodologies for time-series analysis (HANTS algorithm) and a wavelet-based data compression algorithm for hyperspectral images. He participated in several European Space Agency (ESA) studies in preparation for a multiangular hyperspectral Earth Explorer Mission. In 2005, he contributed in the ESA-China DRAGON Program with 12 lectures in Beijing, China. He was appointed as a Visiting Professor at Beijing Capital Normal University. Since May 2006, he has been holding a Visiting Professor position (30%) at the International Institute for Geo-Information Science and Earth Observation ITC, Enschede, The Netherlands. He is a member of ESA's FLEX Mission Assessment Group.

Li Jia received the B.Sc. degree in dynamic meteorology from the Beijing College of Meteorology, Beijing, China, in 1988, the M.Sc. degree in atmospheric boundary-layer physics from the Chinese Academy of Sciences, Beijing, in 1997, and the Ph.D. degree in environmental science from Wageningen University, Wageningen, The Netherlands, in 2004.

Between 1988 and 1999, she was an Assistant Researcher and an Associate Research Professor in the Lanzhou Institute of Plateau Atmospheric Physics, Chinese Academy of Sciences, China. From 2002 to 2004, she had a two-year Postdoctoral Fellowship jointly at the Sub-department of Water Resources, Wageningen University and the Centre for Geo-Information, Alterra Green World Research, The Netherlands. She is currently a Research Scientist in Alterra Green World Research, Wageningen University and Research Centre, Wageningen, The Netherlands. She is a Guest Professor at the School of Geography, Beijing Normal University, China. Her research interests are in the fundamentals of optical remote sensing, application of remote sensing to land-surface processes and global climate and environmental changes, and hydrometeorology.

Qing Xiao received a degree from Jilin University, Changchun, China, in 1993, and the M.Sc. and Ph.D. degrees in remote sensing from the Institute of Remote Sensing Applications, Chinese Academy of Sciences, Beijing, in 1996 and 2002, respectively.

He is currently a Senior Engineer in the Key Laboratory of Remote Sensing, Beijing Research Institute of Uranium Geology, China National Nuclear Corporation, Beijing. He is also a Guest Researcher in the Institute of Remote Sensing Applications, Chinese Academy of Sciences. His research interests are in quantitative processing and application of thermal-infrared emissivity data and information extraction from imaging hyperspectral data.

Z. Su received the B.Sc. degree in hydraulic engineering from the Taiyuan University of Technology, Taiyuan, China, the Postgraduate diploma and the M.Sc. degree (with distinction) in hydrological engineering from the United Nations Educational, Scientific, and Cultural Organization-Institute for Water Education, Delft, The Netherlands, and the Ph.D. degree in civil engineering from Ruhr University, Bochum, Germany.

From 1994 to 1996, he worked as a Postdoctoral Researcher in the Laboratory of Hydrology and Water Management, Faculty of Agriculture and Applied Biological Sciences, University of Ghent, Belgium. He was a Senior Scientist in remote sensing and hydroclimatology at Wageningen University and Research Centre, Alterra Green World Research, before he was with the International Institute of Geo-information Science and Earth Observation ITC in October 2004. He was appointed as a Guest Professor in the School of Water Resources and Environment, China University of Geosciences, Beijing, in 2001, and as a Guest Professor in the Institute for the Tibetan Plateau Research, Chinese Academy of Sciences, in 2005. He is a Professor of spatial hydrology and water-resource management at ITC and Twente University, Enschede, The Netherlands. His current research focuses on remote sensing and numerical modeling of land-surface processes and interactions with the atmosphere, Earth observation of water cycle and applications in climate and ecosystem studies, and monitoring of food security and water-related disasters.